

Longitudinal Stability of Recycler Bunches

Part I: Thresholds for Loss of Landau Damping

T. Sen, C.M. Bhat, and J.-F. Ostiguy

Fermi National Accelerator Laboratory

Batavia, IL 60510

Abstract

We examine the stability of intense flat bunches in barrier buckets used in the Recycler. We consider some common stationary distributions and show that they would be unstable against rigid dipole oscillations. We then discuss an analytical model for the line density that best describes measured bunch profiles. We include space charge in this model to predict the bunch intensity at which Landau damping would be lost. The dependence of this threshold on the bunch length is studied and related to the results of an experimental study with shorter bunch lengths. The threshold for the microwave instability is estimated. These studies will be followed by more detailed numerical studies.

Contents	
I. Introduction	2
II. Single particle dynamics	4
III. Stationary distribution in a barrier bucket	8
A. Binomial distribution	9
B. Elliptic distribution	11
1. Energy distribution	12
C. Exponential distribution	13
IV. Frequency of coherent motion	16
A. Landau damping for an elliptic distribution	17
B. Landau damping for an exponential distribution	19
V. Measured distributions	19
A. Threshold for loss of Landau damping	22
VI. Instability thresholds at different bunch lengths	26
VII. Microwave instability	32
VIII. Conclusions	33
References	34

I. INTRODUCTION

The creation of long flat bunches is under study for the LHC upgrade as a way of increasing the luminosity [1]. The stability of such bunches is one of the key issues of interest. At the Fermilab Recycler [2], long flat bunches are created using rf barriers. At present intensities these bunches are observed to be stable with lifetimes around 20-50 hours (depending on intensity). When electron cooling is enabled, the lifetime

Parameter	Value	Units
Circumference	3331.0	m
Energy	8.93	GeV
Bunch intensity	4.5×10^{12}	
γ_t	19.97	
Rf voltage V_0	1.8	kV
T_1	48.0	$0.0189 \mu \text{ sec}$
T_2	324.0	$0.0189 \mu \text{ sec}$
Bunch area	100.0	eV-sec
ν_s^{max}	9.97×10^{-6}	

TABLE I: Recycler bunch parameters

reaches ~ 500 hours at bunch intensities below 4.5×10^{12} . We explore the longitudinal stability of these bunches at higher intensities [3, 4].

Bunches are confined within a barrier bucket by two voltage pulses of equal magnitude and opposite polarity. The pulses, of equal duration T_1 , are separated by a duration T_2 with no applied voltage. The body of the bunch is contained within the interval T_2 but the head and tail of the bunch penetrate into the barrier on either side. Between the barrier pulses, the beam particles feel no longitudinal focusing force and can be considered to be coasting. Changing T_2 adiabatically changes the bunch length while preserving the bunch area. The main longitudinal parameters of the Recycler bunches are shown in Table I. Single particle dynamics within such a bucket was studied in [5]. Collective effects were numerically studied in the context of a low energy heavy ion ring [6]. Longitudinal stability in the Recycler may be influenced by several factors. For example, the synchrotron period is rather long, hence even slowly growing instabilities which normally would not be of concern can in this case be important. Furthermore, since the bunches are long, they can be excited by relatively low frequency excitations.

In this paper we will consider primarily the thresholds for the loss of Landau damp-

ing and also discuss the results of experiments to determine the impact of a local instability possibly induced at short bunch lengths. In Section II we discuss single particle dynamics in a barrier bucket for the sake of completeness and handy reference. In Section III we consider two stationary distributions that are widely used to describe bunches confined by conventional harmonic rf systems as candidates to describe the Recycler bunches. In Section IV we calculate the coherent frequency of rigid dipole oscillations for these distributions and the relationship to the maximum of the bare incoherent frequency. In Section V we find an analytical distribution that adequately describes the measured profiles. This distribution is then used to calculate the incoherent frequency distribution in the presence of space charge. The intensity threshold at which Landau damping would be lost is predicted while keeping other bunch parameters unchanged. In Section VI we consider the experimental results obtained when the bunch length is changed and discuss the dependence of the threshold for loss of Landau damping. Section VII has a brief discussion of the microwave instability and a rough estimate of the threshold intensity. We conclude in Section VIII. In a subsequent paper we plan to a) discuss the stability diagrams for the Recycler bunches and b) use numerical simulations to study the stability limits in greater detail.

II. SINGLE PARTICLE DYNAMICS

As mentioned above, a barrier bucket consists of two voltage pulses of equal and opposite polarity, each lasting for time T_1 and separated by a time T_2 . The pulses can be of arbitrary shape, rectangular, triangular, half-sinusoidal etc. In most of this report we will consider a rectangular pulse profile.

Let τ be the time delay between an off-energy particle and the synchronous particle which arrives at the center of the bucket $\tau = 0$. The equations of motion are

$$\begin{aligned} \frac{d}{dt}\tau &= -\eta \frac{\Delta E}{\beta^2 E_0} \\ \frac{d}{dt}\Delta E &= \frac{eV(\tau)}{T_0} \end{aligned} \tag{1}$$

Here η is the slip factor, and T_0 the revolution period. Since the bucket is centered at

$\tau = 0$, there is no change of energy for $-T_2/2 \leq \tau \leq T_2/2$. The second order equation of motion for τ is

$$\frac{d^2}{dt^2}\tau + \frac{\eta}{\beta^2 E_0 T_0} eV(\tau) = 0 \quad (2)$$

From the first order equations of motion it follows that the Hamiltonian is

$$H = -\frac{1}{2} \frac{\eta}{\beta^2 E_0} (\Delta E)^2 - \frac{e}{T_0} \int_0^\tau V(s) ds = -\frac{\eta}{2\beta^2 E_0} (\Delta E)^2 - \frac{e}{T_0} U(\tau) \quad (3)$$

where U is the potential function.

At the bucket boundary or separatrix, the bucket height in energy ΔE_{bucket} is determined by

$$H_{bucket} = -\frac{1}{2} \frac{\eta}{\beta^2 E_0} (\Delta E_{bucket})^2 = \frac{e}{T_0} \int_{T_2/2}^{T_2/2+T_1} V(s) ds \quad (4)$$

Hence the bucket height is

$$\Delta E_{bucket} = \left[\frac{2\beta^2 E_0}{T_0} \left| \frac{1}{\eta} \int_{T_2/2}^{T_2/2+T_1} eV(s) ds \right| \right]^{1/2} \quad (5)$$

On any other level curve inside the boundary, the maximum time extent of a particle is $T_2/2 + W$, where the parameter W is the barrier penetration depth for that particle. Then the maximum energy extent of a particle as a function of W is

$$\Delta \hat{E} = \left[\frac{2\beta^2 E_0}{T_0} \left| \frac{1}{\eta} \int_{T_2/2}^{T_2/2+W} eV(s) ds \right| \right]^{1/2} \quad (6)$$

The particle energy deviation stays constant at this value for $-T_2/2 \leq \tau \leq T_2/2$. At other times, the energy deviation can be found from

$$\Delta E(\tau) = \left[(\Delta \hat{E})^2 - \frac{2\beta^2 E_0}{|\eta| T_0} \int_{T_2/2}^{T_2/2+W} eV(s) ds \right]^{1/2} = \left[\frac{2\beta^2 E_0}{|\eta| T_0} \int_{T_2/2+\tau}^{T_2/2+W} eV(s) ds \right]^{1/2} \quad (7)$$

From the first of Equations (1) it follows that the time period on a phase curve is

$$T_s = \frac{\beta^2 E_0}{|\eta|} \left[2 \frac{T_2}{\Delta \hat{E}} + 4 \int_0^W \frac{d\tau}{\Delta E(\tau)} \right] \quad (8)$$

where ΔE in the integral is determined from the expression in Equation (7).

We now specialize to the case of rectangular pulse profiles, i.e. the voltage is given by

$$\begin{aligned}
V(\tau) &= -V_0 & -\left(\frac{1}{2}T_2 + T_1\right) \leq \tau \leq -\frac{1}{2}T_2 \\
&= 0 & -\frac{1}{2}T_2 \leq \tau \leq \frac{1}{2}T_2 \\
&= V_0 & \frac{1}{2}T_2 \leq \tau \leq \frac{1}{2}T_2 + T_1
\end{aligned} \tag{9}$$

The potential which is only determined up to an additive constant can be written as

$$\begin{aligned}
U(\tau) &= -V_0\left[\tau + \frac{1}{2}T_2\right] < 0 & -\left(T_1 + \frac{1}{2}T_2\right) \leq \tau \leq -\frac{1}{2}T_2 \\
&= 0 & -\frac{1}{2}T_2 \leq \tau \leq \frac{1}{2}T_2 \\
&= V_0\left[\tau - \frac{1}{2}T_2\right] > 0 & \frac{1}{2}T_2 \leq \tau \leq \frac{1}{2}T_2 + T_1
\end{aligned} \tag{10}$$

Here we have chosen the additive constant so that the potential also vanishes where the voltage does. The potential is zero outside this range defined above.

For this profile, the peak energy deviation on a phase curve with barrier penetration depth W , the bucket height and the time period on an orbit are

$$\begin{aligned}
\Delta\hat{E} &= \left[2\frac{\beta^2 E_0}{|\eta| T_0} eV_0 W\right]^{1/2}, \\
\Delta E_{bucket} &= \left[2\frac{\beta^2 E_0}{|\eta| T_0} eV_0 T_1\right]^{1/2} \\
T_s &= 2\frac{\beta^2 E_0}{|\eta|} \frac{T_2}{\Delta\hat{E}} + 4\frac{T_0}{eV_0} \Delta\hat{E}
\end{aligned} \tag{11}$$

Note that the period does not go to infinity on the separatrix, as is the case for harmonic rf.

The peak energy offset, at which the period reaches a minimum, is

$$\Delta\hat{E}|_{min T_s} = \left[\frac{\beta^2 E_0 eV_0 T_2}{2|\eta| T_0}\right]^{1/2} = \sqrt{\frac{T_2}{4T_1}} \Delta E_{bucket} \tag{12}$$

This leads to the conclusions that (a) if $T_2 > 4T_1$, the period minimum occurs outside the bucket, i.e. the synchrotron period just decreases monotonically inside the bucket and (b) if $T_2 < 4T_1$, there is a point where the period reaches a minimum and then

increases up to the bucket. The region of zero slope in the period is associated with local loss of Landau damping. This simple stability criterion requires that the interval between pulses be greater than four times the pulse width.

The synchrotron tune on an orbit and the maximum tune when it occurs inside the bucket are respectively

$$\begin{aligned}\nu_s &= \frac{T_0}{T_s} = \left[2 \frac{\beta^2 E_0}{|\eta|} \frac{T_2}{\Delta \hat{E} T_0} + 4 \frac{\Delta \hat{E}}{e V_0} \right]^{-1} = \left(\frac{|\eta| e V_0 T_0}{2 \beta^2 E_0} \right)^{1/2} \frac{\sqrt{W}}{T_2 + 4W} \\ \nu_{s,max} &= \left[\frac{|\eta| e V_0}{32 \beta^2 E_0} \frac{T_0}{T_2} \right]^{1/2}\end{aligned}\quad (13)$$

Note that this maximum tune is independent of the pulse width T_1 .

The peak energy $\Delta \hat{E}$ on a phase curve is related to the barrier penetration depth W by

$$\frac{\Delta \hat{E}}{\Delta E_{bucket}} = \sqrt{\frac{W}{T_1}} \quad (14)$$

The synchrotron tune on a phase curve is related to the maximum tune as

$$\frac{\nu_s}{\nu_{s,max}} = 4 \frac{\kappa}{1 + 4\kappa^2}, \quad \kappa = \sqrt{\frac{W}{T_2}} = \sqrt{\frac{T_1}{T_2}} \frac{\Delta \hat{E}}{\Delta E_{bucket}} \quad (15)$$

where we have defined a dimensionless parameter κ to label a phase curve.

On the phase curve where the synchrotron tune is maximum, $\kappa = 1/2$. At the bucket boundary, it has its maximum value $\kappa_{bucket} = \sqrt{T_1/T_2}$.

Area under phase curve

The phase curve for a rectangular pulse profile consists of straight lines at $\pm \Delta \hat{E}$ between $-T_2/2$ and $T_2/2$ closed by parabolic paths. On these parabolic paths, the relation between the time delay coordinate and the energy deviation is

$$\tau = \frac{\eta T_0}{2 \beta^2 E_0 e V_0} [(\Delta \hat{E})^2 - (\Delta E)^2], \quad (16)$$

while the area under each parabolic path is

$$\int_{-\Delta \hat{E}}^{\Delta \hat{E}} \tau d(\Delta E) = \frac{2}{3} \frac{|\eta| T_0}{\beta^2 E_0 e V_0} (\Delta \hat{E})^3 \quad (17)$$

Hence the area under a phase curve is

$$A = 2\Delta\hat{E}T_2 + \frac{4}{3}\frac{|\eta|T_0}{\beta^2E_0eV_0}(\Delta\hat{E})^3 = 2\Delta\hat{E}T_2\left[1 + \frac{4}{3}\kappa^2\right] \quad (18)$$

while the bucket area is

$$A_{bucket} = 2\Delta E_{bucket}T_2\left[1 + \frac{4}{3}\frac{T_1}{T_2}\right] = 2\left[2\frac{\beta^2E_0}{|\eta|T_0}eV_0T_1\right]^{1/2}T_2\left[1 + \frac{4}{3}\frac{T_1}{T_2}\right] \quad (19)$$

If the maximum energy spread of the bunch $\Delta\hat{E}_{bunch}$ is known, e.g. from a longitudinal Schottky measurement, then the bunch area can be found from Equation (18). Currently the energy spread and the bunch area of the Recycler beam are measured using a 1.7GHz Schottky detector. For a beam with energy spread less than ± 23 MeV, the Schottky frequency spread is less than ± 40 kHz, Hence in practice, the area under the Schottky spectrum between -40 MHz and 40 MHz is calculated, and the energy spread corresponding to 95% of this area is found. This value is used to calculate the bunch area which contains 95% of the particles.

Bunch length

The bunch barrier penetration depth W_b can also be determined from the maximum energy spread in the bunch using Equation (14), i.e. $W_b = (\Delta\hat{E}_{bunch}/\Delta E_{bucket})^2T_1$. The bunch length is $\tau_b = T_2/2 + W_b$. These equations express the fact that larger initial energy spread in the bunch lead to deeper barrier penetration.

III. STATIONARY DISTRIBUTION IN A BARRIER BUCKET

The time evolution of the phase space density ρ follows from

$$\frac{d\rho}{dt} = \frac{\partial\rho}{\partial t} + \{\rho, H\} \quad (20)$$

If the density is not explicitly time dependent and it is a function of the Hamiltonian H so that the Poisson bracket $\{\rho, H\}$ vanishes, then the density is stationary.

Due to the symmetry of the barrier, the phase curves are also symmetrical, each phase curve extending from $-W - 0.5T_2$ to $W + 0.5T_2$ on the τ axis (this defines W)

and from $-\Delta\hat{E}$ to $\Delta\hat{E}$ on the energy axis. The peak energy $\Delta\hat{E}$ on a phase curve can be found from

$$(\Delta\hat{E})^2 = \frac{2\beta^2 E_0 e}{|\eta| T_0} \int_{0.5T_2}^{0.5T_2+W} V(s) ds = \frac{2\beta^2 E_0 e}{|\eta| T_0} [U(\frac{1}{2}T_2 + W) - U(\frac{1}{2}T_2)] \quad (21)$$

At the bunch boundary on the τ axis $\tau = \tau_b$ and $\Delta E = 0$, and the Hamiltonian takes on the value

$$H = H_b = -\frac{e}{T_0} U(\tau_b) \equiv -\frac{e}{T_0} U_b \quad (22)$$

written in terms of the potential function U_b at $\tau = \tau_b$.

A. Binomial distribution

Consider a general binomial distribution for the density

$$\rho(\Delta E, \tau) = c_1 [H_b - H]^p \quad (23)$$

where p is a real number and c_1 is the normalization constant.

The density can be expanded to the form

$$\begin{aligned} \rho(\Delta E, \tau) &= c_1 \left[\frac{\eta}{2\beta^2 E_0} \right]^p \left[\frac{2\beta^2 E_0 e}{\eta T_0} [U(\tau) - U_b] - \Delta E^2 \right]^p \\ &= c_1 \left[\frac{\eta}{2\beta^2 E_0} \right]^p [\Delta E_b(\tau)^2 - \Delta E^2]^p \end{aligned} \quad (24)$$

where we have used the fact that at any point on the bunch boundary, the energy deviation can be found from

$$\Delta E_b(\tau)^2 = \frac{2\beta^2 E_0 e}{|\eta| T_0} [U(\tau) - U_b] \quad (25)$$

The line density is obtained by projecting the phase space density on to the τ axis,

$$\lambda(\tau) = \int_{-\Delta E_b(\tau)}^{\Delta E_b(\tau)} \rho(\Delta E, \tau) d(\Delta E) = 2c_1 \left[\frac{\eta}{2\beta^2 E_0} \right]^p \int_0^{\Delta E_b(\tau)} [\Delta E_b(\tau)^2 - \Delta E^2]^p \quad (26)$$

where in the second equality we have used the fact that the integrand is even. Using the integration result

$$\int_0^{\Delta E_b} [\Delta E_b^2 - \Delta E^2]^p d(\Delta E) = \frac{\Gamma(p+1)}{\Gamma(p+3/2)} [\Delta E_b(\tau)]^{2p+1}$$

we obtain for the line density

$$\lambda(\tau) = \lambda_0 [U(\tau) - U_b]^{p+1/2}, \quad \lambda_0 = N_b \left[\int_{-\tau_b}^{\tau_b} (U(\tau) - U_b)^{p+1/2} d\tau \right]^{-1} \quad (27)$$

where we have absorbed the constant c_1 and the other parameters into a new constant λ_0 .

The distortion of the potential due to external inductive impedances and space charge can be included with the concept of an effective impedance. The effective impedance at frequency ω is defined as

$$\frac{Z_{eff}}{n} = i(\omega_0 L - \frac{g_0 Z_0}{2\beta\gamma^2}) \equiv i\omega_0 L_{eff} \quad (28)$$

where $n = \omega/\omega_0$ is the harmonic of the revolution frequency, L is the inductive impedance of the machine, $Z_0 = 377\Omega$ is the vacuum impedance. The geometric space charge factor g_0 for a round beam in a round beam pipe is given by

$$g_0 = \frac{1}{2} + 2 \ln(b/a) \quad (29)$$

where b is the radius of the beam-pipe and a is the beam radius.

The induced voltage due to this impedance is

$$V_{ind} = -L_{eff} \frac{dI}{dt} = -L_{eff} \frac{dI}{d\tau} \quad (30)$$

From the bunch current $I(\tau) = e\lambda(\tau)$, it follows that for a binomial distribution,

$$\frac{dI}{d\tau} = e\lambda_0 \left(p + \frac{1}{2}\right) [U(\tau) - U_b]^{p-\frac{1}{2}} V(\tau) \quad (31)$$

Introducing the notation

$$u(-\tau_b, \tau_b) = \int_{-\tau_b}^{\tau_b} [U(\tau) - U_b]^{p+\frac{1}{2}} d\tau \quad (32)$$

the induced voltage can be written as

$$V_{ind} = -\frac{eN_b \left(p + \frac{1}{2}\right)}{\omega_0 u(-\tau_b, \tau_b)} \text{Im} \left[\frac{Z_{eff}}{n} \right] [U(\tau) - U_b]^{p-\frac{1}{2}} V(\tau) \quad (33)$$

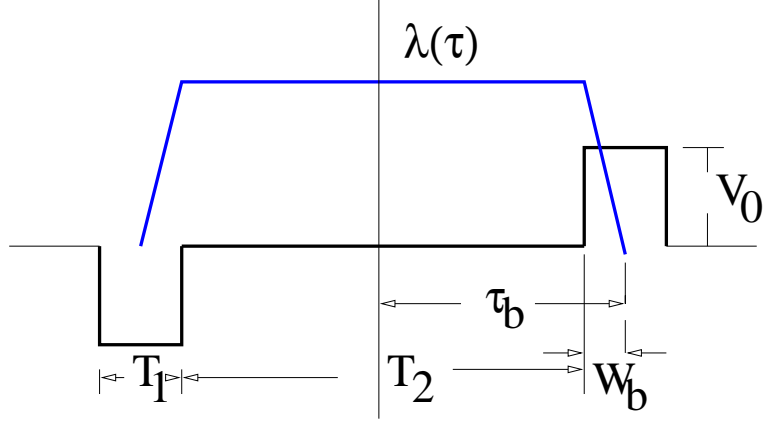


FIG. 1: Rectangular barrier bucket voltage profile and the line density (in blue) in a stationary elliptic distribution. T_1 is the width of each pulse, T_2 is the duration between the pulses, τ_b is half the bunch length and W_b is the barrier penetration depth.

B. Elliptic distribution

The elliptic distribution is obtained by choosing $p = 1/2$ which yields

$$\lambda(\tau) = \lambda_0[U(\tau) - U_b] \quad (34)$$

As we will see, this distribution has some special properties, first pointed out by Hofmann and Pedersen [7].

The line density for an elliptic distribution with boundaries at $(-\tau_b, \tau_b)$ is

$$\lambda(\tau) = \lambda_0[U(\tau) - U(\tau_b)] = \frac{N_b}{u(-\tau_b, \tau_b)}[U(\tau) - U(\tau_b)] \quad (35)$$

Hence the stationary elliptic distribution in this rectangular barrier bucket is

$$\begin{aligned} \lambda(\tau) &= \frac{N_b}{[\tau_b^2 - (\frac{1}{2}T_2)^2]}(\tau + \tau_b) & -\tau_b \leq \tau \leq -\frac{1}{2}T_2 \\ &= \frac{N_b}{[\tau_b^2 - (\frac{1}{2}T_2)^2]}(\tau_b - \frac{1}{2}T_2) & -\frac{1}{2}T_2 \leq \tau \leq \frac{1}{2}T_2 \\ &= -\frac{N_b}{[\tau_b^2 - (\frac{1}{2}T_2)^2]}(\tau - \tau_b) & \frac{1}{2}T_2 \leq \tau \leq \tau_b \end{aligned} \quad (36)$$

This has a trapezoidal shape as shown in Figure 1.

For an elliptic distribution the induced voltage is

$$V_{ind} = -\frac{eN_b}{\omega_0 u(-\tau_b, \tau_b)} \text{Im}\left[\frac{Z_{eff}}{n}\right] V(\tau) \quad (37)$$

In this case it has the same form as the rf voltage so the total voltage is related to the focusing rf voltage by a change of scale. The total voltage is

$$V_t(\tau) = V(\tau) + V_{ind}(\tau) = \left\{ 1 - \frac{eN_b}{\omega_0 u(-\tau_b, \tau_b)} \text{Im}\left[\frac{Z_{eff}}{n}\right] \right\} V(\tau) \quad (38)$$

By definition of the voltage waveform, a synchronous particle sees no focusing voltage. Hence the ratio of the total focusing voltage to the rf focusing voltage is

$$k_t = \frac{V_t}{V} = 1 - \frac{eN_b}{\omega_0 u(-\tau_b, \tau_b)} \text{Im}\left[\frac{Z_{eff}}{n}\right] \quad (39)$$

The maximum synchrotron tune in the presence of space charge and external impedances is

$$\nu_s^{max} = \left[\frac{eV_t |\eta| T_0}{32\beta^2 E_0 T_2} \right]^{1/2} = \sqrt{k_t} \nu_{s,0}^{max} \quad (40)$$

where $\nu_{s,0}^{max}$ is the maximum tune in the absence of space charge and external impedances. Similarly the area under a phase curve with turning points (τ_1, τ_2) on the τ axis is given by

$$A_t(\tau_1, \tau_2) = \sqrt{k_t} A(\tau_1, \tau_2) \quad (41)$$

The area of the bucket is reduced by the factor $\sqrt{k_t^{bucket}}$ given by Equation (39) with $\tau_b = 0.5T_2 + T_1$. The maximum theoretical intensity that can be stored in the bucket corresponds to the case where the space charge and external impedances distort the potential sufficiently to reduce the bucket area to zero. In practice, the limiting bunch intensity will be lower than this value, for example when the reduced bucket area can just accommodate the longitudinal emittance of bunches from the Booster.

1. Energy distribution

The energy distribution can be found by projecting the phase space density on to the energy axis. Let $\mu(\Delta E)$ represent the energy distribution, then

$$\mu(\Delta E) \equiv \int \rho(\Delta E, \tau) d\tau = c_1 \left[\frac{|\eta|}{2\beta^2 E_0} \right]^{1/2} \int_{-\tau_b}^{\tau_b} [|\Delta E_b^2(\tau) - \Delta E^2|]^{1/2} \quad (42)$$

Note that μ is even in the energy. The energy offset on the bunch boundary is defined in Equation (25). Over the three regions we have

$$\begin{aligned}
\Delta E_b^2(\tau) &= -\Delta E_{bucket}^2 \frac{\tau + \tau_b}{T_1} & -\tau_b \leq \tau \leq -\frac{1}{2}T_2 \\
&= -\Delta E_{bucket}^2 \frac{\tau_b - \frac{1}{2}T_2}{T_1} & -\frac{1}{2}T_2 \leq \tau \leq \frac{1}{2}T_2 \\
&= \Delta E_{bucket}^2 \frac{\tau - \tau_b}{T_1} & \frac{1}{2}T_2 \leq \tau \leq \tau_b
\end{aligned} \tag{43}$$

Consequently

$$\begin{aligned}
\mu(\Delta E) &= c_1 \left[\frac{eV_0}{T_0} \right]^{1/2} \left\{ \int_{-\tau_b}^{-T_2/2} \left| \tau + \tau_b - T_1 \frac{\Delta E^2}{\Delta E_{bucket}^2} \right|^{1/2} d\tau + \left| \tau_b - \frac{1}{2}T_2 - T_1 \frac{\Delta E^2}{\Delta E_{bucket}^2} \right|^{1/2} T_2 \right. \\
&\quad \left. + \int_{T_2/2}^{\tau_b} \left| -\tau + \tau_b - T_1 \frac{\Delta E^2}{\Delta E_{bucket}^2} \right|^{1/2} d\tau \right\} \\
&= c_1 \left[\frac{eV_0 T_1}{T_0} \right]^{1/2} \left\{ T_2 \left| \frac{\Delta E^2}{\Delta E_{bucket}^2} - \frac{W_b}{T_1} \right|^{1/2} - \frac{4}{3} T_1 \left[\left| \frac{\Delta E}{\Delta E_{bucket}} \right|^3 - \left| \frac{\Delta E^2}{\Delta E_{bucket}^2} - \frac{W_b}{T_1} \right|^{3/2} \right] \right\}
\end{aligned} \tag{44}$$

This has its maximum at $\Delta E = 0$ and vanishes at

$$\Delta E_{max} = \pm \Delta E_{bucket} \left[b + \frac{1}{2a(2-3ab)} [3a^2b^2 - 1 + \sqrt{(3a^2b^2 - 1)^2 + 4a^3b^3(2-3ab)}] \right]^{1/2} \tag{45}$$

where $a = (4/3)T_1/T_2$, $b = W_b/T_1$. For the Recycler parameters shown in Table I, this yields a vanishing of the energy distribution at ± 7.87 MeV well below the bucket height $\Delta E_{bucket} = 17.38$ MeV.

A sketch of the density distribution is shown in Figure 2, the parameters are those of the Recycler. The plotted density is normalized to its maximum value at $\Delta E = 0$. As is the case for the line density, there is a well defined value beyond which the distribution $\mu(E)$ vanishes.

C. Exponential distribution

The energy distribution for the elliptic phase space distribution does not match the approximately Gaussian energy distribution that is observed in the longitudinal

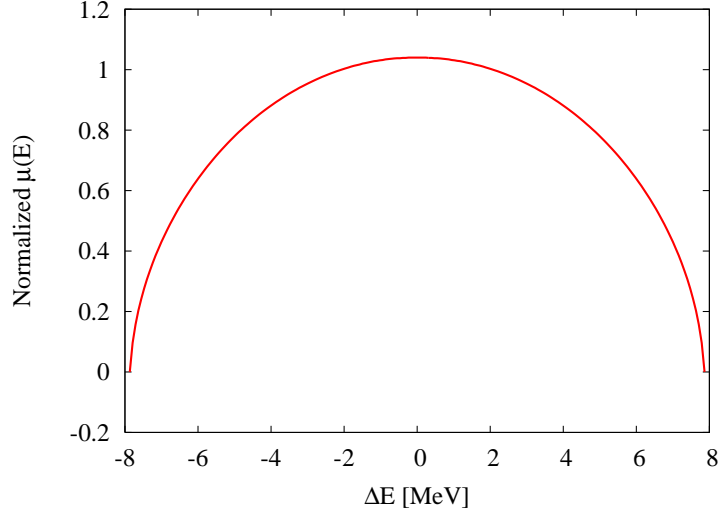


FIG. 2: The energy distribution as a function of the energy spread, for the Recycler parameters, assuming an elliptic phase space distribution.

Schottky spectrum of Recycler bunches. We therefore consider another distribution which naturally leads to a Gaussian energy distribution. Consider the density to be an exponential function of the Hamiltonian.

$$\rho(H) = \rho_0 \exp[H/H_0] = \rho_0 \exp\left\{\frac{1}{H_0} \left[\frac{-\eta}{2\beta^2 E_0} (\Delta E)^2 - \frac{eU(\tau)}{T_0} \right]\right\} \quad (46)$$

The line density obtained by projecting the density onto the time axis is

$$\lambda(\tau) = \int \rho(\Delta E, \tau) d\Delta E = \lambda_0 \exp\left[-\frac{eU(\tau)}{H_0 T_0}\right] \quad (47)$$

where λ_0 is a normalization constant and H_0 is a scale constant to be defined later. From the expression in Eq (10) for the potential function in a rectangular barrier bucket, it follows that the line density for this distribution is

$$\begin{aligned} \lambda(\tau) &= \lambda_0 \exp\left[\frac{eV_0}{H_0 T_0} \left(\tau + \frac{1}{2}T_2 + T_1\right)\right] & - (T_1 + \frac{1}{2}T_2) \leq \tau \leq -\frac{1}{2}T_2 \\ &= \lambda_0 \exp\left[\frac{eV_0}{H_0 T_0} T_1\right] & -\frac{1}{2}T_2 \leq \tau \leq \frac{1}{2}T_2 \\ &= \lambda_0 \exp\left[-\frac{eV_0}{H_0 T_0} \left(\tau - \frac{1}{2}T_2 - T_1\right)\right] & \frac{1}{2}T_2 \leq \tau \leq \frac{1}{2}T_2 + T_1 \end{aligned} \quad (48)$$

Figure 3 shows a sketch of the distribution.

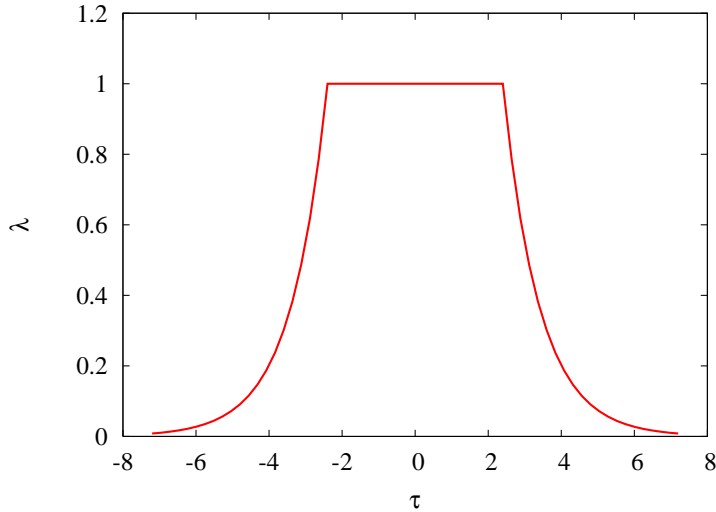


FIG. 3: Sketch of the line density for an exponential distribution. Parameters are arbitrary.

Note that the density does not exactly vanish at τ_b , instead $\lambda(-\tau_b) = \lambda(\tau_b) = \lambda_0 \exp[-(eV_0[T_1 - W_b])/(H_0T_0)]$ where as before $W_b = \tau_b - \frac{1}{2}T_2$. If $eV_0[T_1 - W_b]/(H_0T_0) \gg 1$, then the density is small and can be effectively taken to vanish at $\tau = \tau_b$.

Since the density does not exactly vanish at $\pm\tau_b$, it would be more accurate to extend the region of non-zero density to the entire extent of the barrier bucket. In that case the normalization condition is $\int_{-(T_1+\frac{1}{2}T_2)}^{T_1+\frac{1}{2}T_2} \lambda(\tau)d\tau = N_b$ which yields

$$N_b = \lambda_0 \left[\frac{2H_0T_0}{eV_0} (1 - \exp[-\frac{eV_0T_1}{H_0T_0}]) + T_2 \right] \quad (49)$$

If the line density is known in the flat region, e.g. at the center $\tau = 0$, then from the expression for the line density in Eq (48) above, it follows that the normalization constant is known, i.e. $\lambda_0 = \lambda(\tau = 0)$ and the normalization condition can be used to find the scale constant H_0 . It is simpler here to determine this constant from the energy distribution which in this case is a Gaussian

$$\mu(\Delta E) \equiv \int d\tau \rho(\Delta E, \tau) = \mu_0 \exp[-\frac{(\Delta E)^2}{2\sigma_E^2}] \quad (50)$$

where the rms energy deviation $\sigma_E^2 = \beta^2 E_0 H_0 / \eta$. If the rms energy deviation is measured from the Schottky spectrum, then H_0 is known.

The line density written above is not self-consistent as it does not take into account the potential well distortion due to space charge. Including this intensity dependent effect, the line density is

$$\begin{aligned}\lambda(\tau) &= \lambda_0 \exp\left[-\frac{eU_t(\tau)}{H_0 T_0}\right] \\ U_t(\tau) &= U_{rf}(\tau) + \int_0^\tau V_{ind}(s) ds = U_{rf}(\tau) + \frac{e}{\omega_0} \text{Im}\left[\frac{Z_{eff}}{n}\right][\lambda(0) - \lambda(\tau)]\end{aligned}\quad (51)$$

It follows that the density at time $\tau = 0$ is $\lambda(0) = \lambda_0 \exp[-eU_{rf}(0)/(H_0 T_0)]$. Since we have defined the rf potential such that $U_{rf}(0) = 0$, it follows that $\lambda(0) = \lambda_0$. Hence the self-consistent density is the solution of the following equation

$$\lambda(\tau) \exp\left[-\frac{e^2}{2\pi H_0} \text{Im}\left[\frac{Z_{eff}}{n}\right] \lambda(\tau)\right] = \lambda_0 \exp\left[-\frac{e^2}{2\pi H_0} \text{Im}\left[\frac{Z_{eff}}{n}\right] \lambda_0\right] \exp\left[-\frac{eU_{rf}(\tau)}{H_0 T_0}\right] \quad (52)$$

This is the equivalent of the Hassinski equation which defines a self-consistent stationary solution for a sinusoidal rf and an arbitrary wake field. This equation can be solved numerically to find the self-consistent density at a given intensity. At low intensities this solution will reduce to the form in Equation (48).

IV. FREQUENCY OF COHERENT MOTION

Imagine that the bunch is displaced from its center by $\Delta\tau$ as a result of which it starts to perform small amplitude oscillations. If we let $\bar{\lambda}(\tau)$ be the line density of the displaced bunch, then it follows that $\bar{\lambda}(\tau) = \lambda(\tau - \Delta\tau)$. The infinitesimal force on a slice of thickness $\delta\tau$ is

$$dF = -\frac{e}{\beta c} \lambda(\tau - \Delta\tau) d\tau \frac{\partial U}{\partial \tau} \quad (53)$$

The total force on the bunch is

$$\begin{aligned}F &= -\frac{e}{\beta c} \int_{-\tau_b + \Delta\tau}^{\tau_b + \Delta\tau} \lambda(\tau - \Delta\tau) \frac{\partial U}{\partial \tau} d\tau \\ &= \frac{e}{\beta c} \Delta\tau \int_{-\tau_b}^{\tau_b} \lambda'(\tau) \frac{\partial U}{\partial \tau} d\tau + O[(\Delta\tau)^2]\end{aligned}\quad (54)$$

where we have expanded the displaced density to first order in $\Delta\tau$ and used the fact that the average force on the undisplaced bunch vanishes. From the equation of motion

and the force law $F \equiv -eV(\tau)/(\beta c) = m_{eff}\ddot{\tau}$, it follows that the effective mass of a particle is $m_{eff} = \beta E_0 T_0 / (c\eta)$ and hence the effective mass of the bunch is $m_{eff}^{bunch} = N_b \beta E_0 T_0 / (c\eta)$. If the centroid is oscillating at a frequency ω_c , then from the small amplitude equation of motion $F/m_{eff}^{bunch} \equiv \ddot{\tau}_c = -\omega_c^2 \Delta\tau$, it follows that the coherent frequency is

$$\omega_c^2 = \frac{e|\eta|}{\beta^2 E_0 T_0 N_b} \int_{-\tau_b}^{\tau_b} \lambda'(\tau) \frac{\partial U}{\partial \tau} d\tau \quad (55)$$

This coherent frequency is independent of intensity. It turns out that for parabolic bunches in a single harmonic rf potential, the coherent frequency and the small amplitude incoherent frequency coincide. In general these frequencies are not the same for other distributions and other rf systems.

A. Landau damping for an elliptic distribution

We will consider the rigid dipole mode to be Landau damped if the frequency of the rigid dipole mode is within the band of incoherent synchrotron frequencies and undamped if it lies outside this band. First we evaluate the coherent dipole frequency for an elliptic distribution. Using the line density of a matched binomial distribution, the coherent frequency using Eq. (55) is

$$\omega_c^2 = \frac{e|\eta|(p + \frac{1}{2})}{\beta^2 E_0 T_0 u(-\tau_b, \tau_b)} \int_{-\tau_b}^{\tau_b} [U(\tau) - U(\tau_b)]^{p-1/2} \left(\frac{\partial U}{\partial \tau}\right)^2 d\tau \quad (56)$$

This frequency, in the absence of external forces, is independent of the bunch intensity. For the elliptic distribution this reduces to

$$\omega_c^2 = \frac{e|\eta|}{\beta^2 E_0 T_0 u(-\tau_b, \tau_b)} \int_{-\tau_b}^{\tau_b} V^2(\tau) d\tau = \frac{2eV_0|\eta|}{\beta^2 E_0 T_0 (\tau_b + \frac{1}{2}T_2)} \quad (57)$$

As remarked above, the total focusing voltage is changed by space charge and external impedances. For an elliptic distribution, the total voltage is related to the rf voltage by the factor k_t calculated above and the synchrotron frequency is related to the bare synchrotron frequency by $\sqrt{k_t}$. In a barrier bucket, the incoherent frequency as a function of amplitude rises from zero at the origin to a maximum value which may occur at an amplitude within the bucket. The maximum bare incoherent synchrotron

angular frequency $\omega_{s,0}^{max}$ can be found from Equation (13). In the presence of space charge and external impedances it is modified to

$$\omega_s^{max} = \sqrt{k_t} \omega_{s,0}^{max} = \left[1 + \frac{eN_b \text{Im}(Z_{eff}/n)}{\omega_0 V_0 [\tau_b^2 - (\frac{1}{2}T_2)^2]}\right]^{1/2} \omega_{s,0}^{max} \quad (58)$$

In terms of the bare maximum frequency $\omega_{s,0}^{max}$, the coherent frequency can be written as

$$\omega_c = \frac{4}{\pi} \left[\frac{T_2}{\tau_b + \frac{1}{2}T_2}\right]^{1/2} \omega_{s,0}^{max} \quad (59)$$

Writing $\tau_b = T_2/2 + W_b$, where W_b can be considered as the barrier penetration depth of the bunch, the requirement that the coherent frequency be less than the maximum bare incoherent tune is $W_b/T_2 \geq \frac{16}{\pi^2} - 1$.

Below transition with space charge as the dominant impedance, the net focusing voltage is reduced and the incoherent frequency decreases with intensity. At the threshold for the loss of Landau damping, the maximum incoherent frequency equals the coherent dipole frequency and falls below it at higher intensities. The threshold intensity for the loss of Landau damping found by equating ω_s^{max} and ω_c is

$$N_b^{thresh} = -\frac{\omega_0 V_0 (\tau_b^2 - (\frac{1}{2}T_2)^2)}{e \text{Im}(Z_{eff}/n)} \left[1 - \left(\frac{4}{\pi}\right)^2 \frac{T_2}{\tau_b + \frac{1}{2}T_2}\right] \quad (60)$$

Putting in numbers for the Recycler, we find that

$$\frac{\omega_c}{\omega_s^{max}} = 1.25 \quad (61)$$

This says that even at zero intensity, the coherent frequency would be outside the incoherent band. As the intensity increases, the incoherent frequencies will decrease and the ratio above will increase. Hence there would be no Landau damping at any intensity. We conclude that this distribution cannot be suitable to describe the Recycler longitudinal density.

B. Landau damping for an exponential distribution

The coherent frequency can be found using Eq (55) except that we now extend the region of integration so

$$\omega_c^2 = \frac{e|\eta|}{\beta^2 E_0 T_0 N_b} \int_{-(\frac{1}{2}T_2+T_1)}^{\frac{1}{2}T_2+T_1} \lambda'(\tau) \frac{\partial U}{\partial \tau} d\tau \quad (62)$$

We find

$$\omega_c^2 = \frac{2eV_0|\eta|}{\beta^2 E_0 T_0} \frac{1 - \exp[-\frac{eV_0 T_1}{H_0 T_0}]}{2 \frac{H_0 T_0}{eV_0} (1 - \exp[-\frac{eV_0 T_1}{H_0 T_0}]) + T_2} \quad (63)$$

Expressed in terms of the maximum of the bare incoherent frequency $\omega_{s,0}^{max}$,

$$\frac{\omega_c}{\omega_{s0,max}} = \frac{4}{\pi} \left[\frac{1 - \exp(-\chi W_b)}{1 + (2/(\chi T_2)) [1 - \exp(-\chi W_b)]} \right]^{1/2}, \quad \chi = \beta^2 E_0 e V_0 / (|\eta| \sigma_E^2 T_0) \quad (64)$$

Putting in the Recycler numbers we find that in this case

$$\frac{\omega_c}{\omega_{s0,max}} = 1.27 \quad (65)$$

This distribution is also unsuitable.

V. MEASURED DISTRIBUTIONS

During a study in April 2009, protons were injected into the Recycler with a increasing number of Booster batches. The bunch profiles were measured with a wall current monitor at three different intensities. Longitudinal Schottky spectra were also recorded. The measured bunch length profiles are well described by the function

$$\begin{aligned} \lambda_{fit}(\tau) &= N_b a \{ [1 + \tanh(b\tau + c)] \theta(-\tau) + [1 - \tanh(b\tau - c)] \theta(\tau) \} \\ \lambda_{fit}(0) &= N_b a (1 + \tanh c) \end{aligned} \quad (66)$$

Here θ is the step function, a, b, c are the three parameters of the fit. a sets the overall normalization for the density, b is a measure of the slope in the rising and falling regions and the width of each half section is directly proportional to c . Note that the same parameters describe both the head and the tail of the profile, implying perfect symmetry about the center.

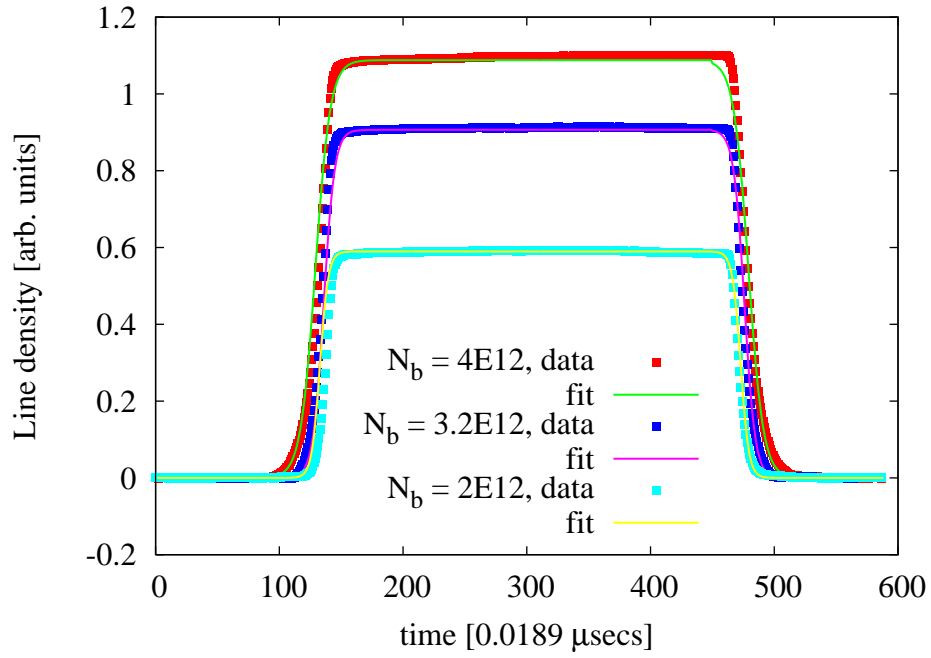


FIG. 4: Comparison of the measured line density and fit to the data with a tanh profile at three different intensities .

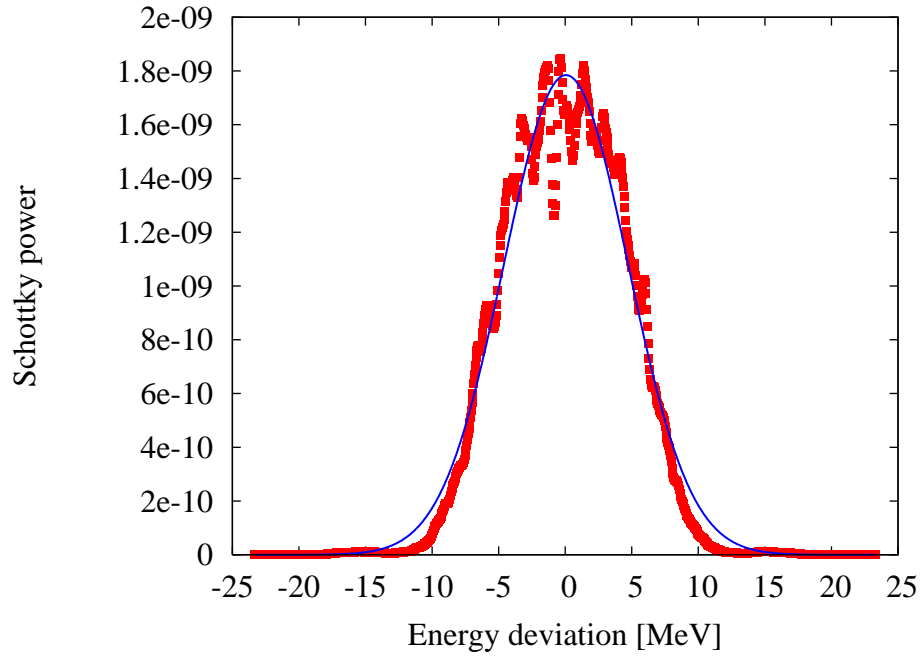


FIG. 5: Measured Schottky power of a proton beam in the Recycler compared with a Gaussian fit.

The measured profiles and the fit function are shown for all three sets in Figure 4. This fitted function appears to describe the measured profiles with very good accuracy. Note that the same fit works equally well at all the intensities suggesting that distortion due to intensity effects are not yet important at these levels. This also suggests that the *tanh* fit is probably not the result of a self-consistent solution to the ‘‘Hassinski equation’’ (52), the assumption being that the fit is also good for lower intensities than those measured here. There is some bunch lengthening as the intensity increases showing the impact of the capacitive space charge impedance.

The line density can also be calculated as a function of the incoherent synchrotron tune. Figure 6 shows the density relative to the density at the center as a function of ν_s^0 , the bare incoherent tune. The Main Injector ramping frequency is also shown in this figure; beam particles resonant with this frequency can be driven to larger amplitudes and lost. However the relative density at this frequency is about 2%, the net effect due to this resonance should be small at present parameters.

We can now use this form of the line density to calculate the coherent frequency. From the expression for the coherent frequency in Equation (55)

$$\begin{aligned}\omega_c^2 &= \frac{|\eta| eV_0}{\beta^2 E_0 T_0 N_b} \left\{ -\left[\lambda\left(-\frac{1}{2}T_2\right) - \lambda(-\tau_b) \right] + \left[\lambda(\tau_b) - \lambda\left(\frac{1}{2}T_2\right) \right] \right\} \\ &= \frac{2|\eta| eV_0 a}{\beta^2 E_0 T_0} \left\{ \tanh(b\tau_b - c) - \tanh\left(\frac{1}{2}bT_2 - c\right) \right\}\end{aligned}\quad (67)$$

Hence the ratio of the coherent frequency to the maximum of the bare incoherent frequency is

$$\frac{\omega_c}{\omega_{s0,max}} = \frac{4}{\pi} \sqrt{aT_2} \sqrt{\tanh[b\tau_b - c] - \tanh\left[\frac{1}{2}bT_2 - c\right]}\quad (68)$$

Here we use the value of the parameter a determined by the normalization condition, i.e.

$$a = \frac{1}{2} \left[\frac{1}{2}T_2 + T_1 + \frac{1}{b} \log\left(\frac{\cosh c}{\cosh[b(T_2/2 + T_1) - c]}\right) \right]^{-1}\quad (69)$$

Using the values of the fit parameters b, c for the data measured in the April 2009 study we find that

$$\frac{\omega_c}{\omega_s^{max}} = 0.93\quad (70)$$

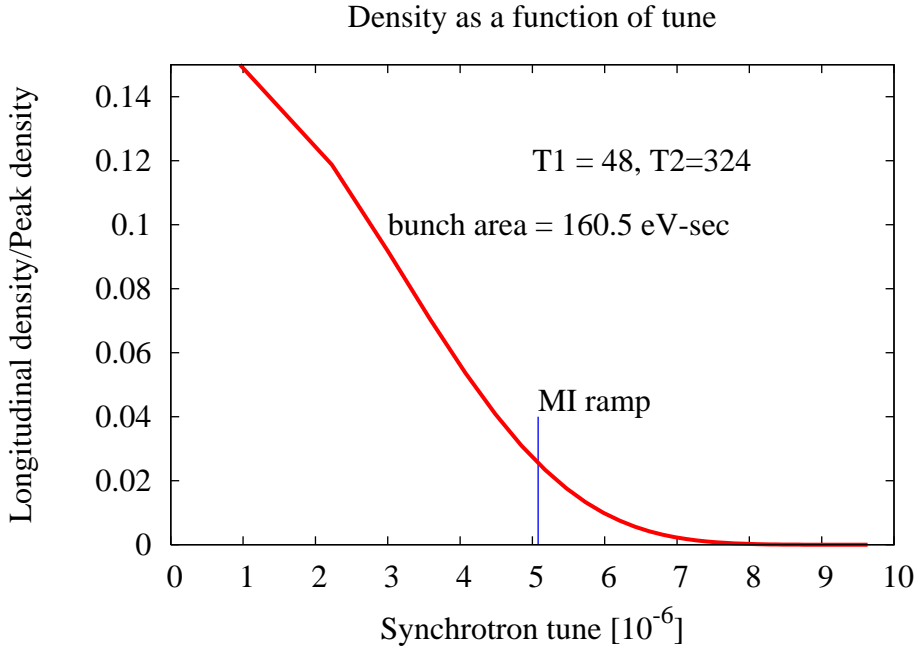


FIG. 6: The relative density as a function of the bare incoherent tune. Most particles have zero tune. For comparison, the tune corresponding to the frequency (0.45 Hz) of the Main Injector ramp is also shown.

i.e. at zero intensity the coherent frequency is within the incoherent spread. Figure 7 shows the coherent tune for the three distributions considered here and the bare incoherent tune as a function of the parameter W .

A. Threshold for loss of Landau damping

We can now take into account the potential well distortion due to space charge and find the incoherent tune in the presence of space charge. The total voltage for an arbitrary distribution is

$$V_t = V_0 - \frac{e}{\omega_0} \text{Im} \left(\frac{Z_{eff}}{n} \right) \frac{d\lambda}{dt} \quad (71)$$

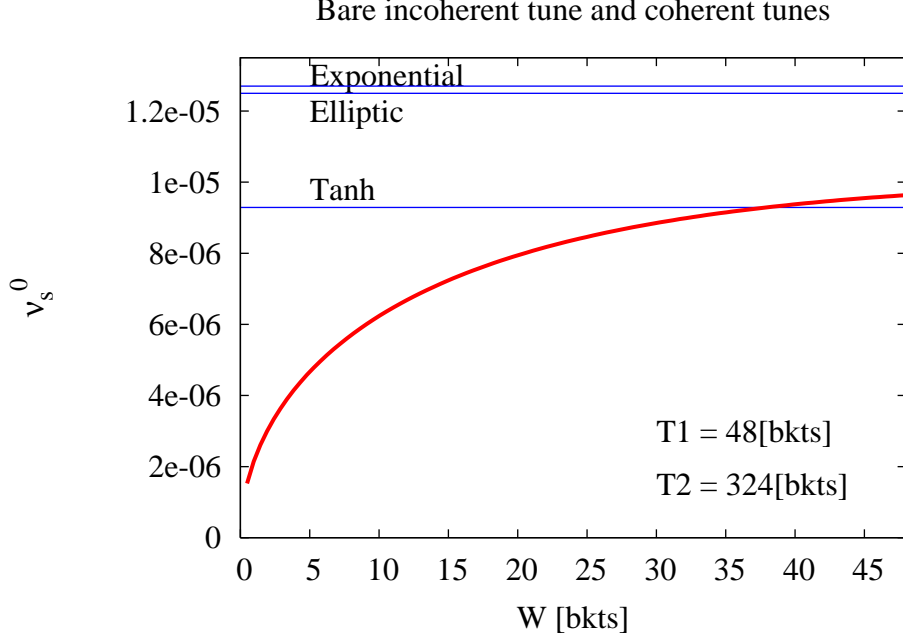


FIG. 7: Bare synchrotron tune vs W , the barrier penetration parameter for each orbit. Also shown are the coherent tunes of the dipole mode for three distributions. The coherent mode would be damped only for the Tanh distribution.

The energy deviation on a curve with barrier penetration W at time τ is

$$\begin{aligned}
 (\Delta E)^2(\tau; W) &= \frac{2\beta^2 E_0}{|\eta| T_0} \int_{T_2/2+\tau}^{T_2/2+W} eV_t(s) ds \\
 &= \frac{2\beta^2 e E_0}{|\eta| T_0} \left\{ V_0(W - \tau) - \frac{e}{\omega_0} \text{Im} \left(\frac{Z_{eff}}{n} \right) \left[\lambda \left(\frac{1}{2} T_2 + W \right) - \lambda \left(\frac{1}{2} T_2 + \tau \right) \right] \right\} \quad (72)
 \end{aligned}$$

Introducing the function $f(W)$ and the parameters ζ, d as

$$f(W) = W + \zeta \tanh(bW + d), \quad \zeta = \frac{e}{\omega_0 V_0} \text{Im} \left(\frac{Z_{eff}}{n} \right) N_b a, \quad d = \frac{1}{2} b T_2 - c \quad (73)$$

we can write

$$(\Delta E)^2(\tau; W) = \frac{2\beta^2 e V_0 E_0}{|\eta| T_0} [f(W) - f(\tau)] \quad (74)$$

while the peak energy is found from $\Delta \hat{E} = \Delta E(0, W)$. The intensity dependence is contained in the parameter ζ .

As the intensity increases, the bucket height and bucket area decrease. A threshold for the maximum intensity that can be stored in the bucket is set when the bucket area

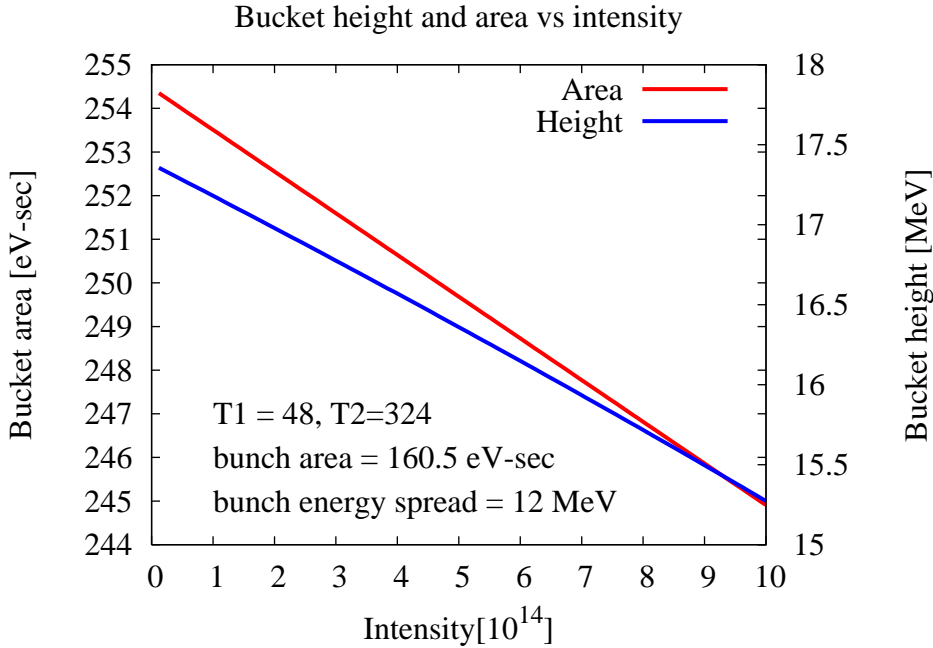


FIG. 8: The bucket area and bucket height as a function of the bunch intensity. Over the range of intensities plotted, the bucket values of the area and height stay well above the initial bunch area and bunch energy spread.

falls to the initial bunch area. Figure 8 shows that at intensities even up to 200 times larger than present, the bucket area and height are larger than the initial bunch area and energy spread respectively. The threshold is at an intensity of 2.3×10^{15} , where the bucket height equals the initial bunch energy spread of 12 MeV.

The incoherent synchrotron tune as a function of W can then be found using Eq (8) as

$$\nu_s(W) = \left(\frac{|\eta| e V_0 T_0}{2\beta^2 E_0} \right)^{1/2} \left[\frac{T_2}{[f(W) - \zeta \tanh d]^{1/2}} + 2 \int_0^W \frac{d\tau}{[f(W) - \tau - \zeta \tanh(b\tau + d)]^{1/2}} \right]^{-1} \quad (75)$$

The integral in the above expression can be performed numerically. For comparison, the bare synchrotron tune without space charge is given in Equation (13).

The top plot in Figure 9 shows the relative difference of the incoherent tunes with and without space charge at intensities varying over two orders of magnitude. The relative tune depression due to space charge is the largest at the inner edge of the voltage

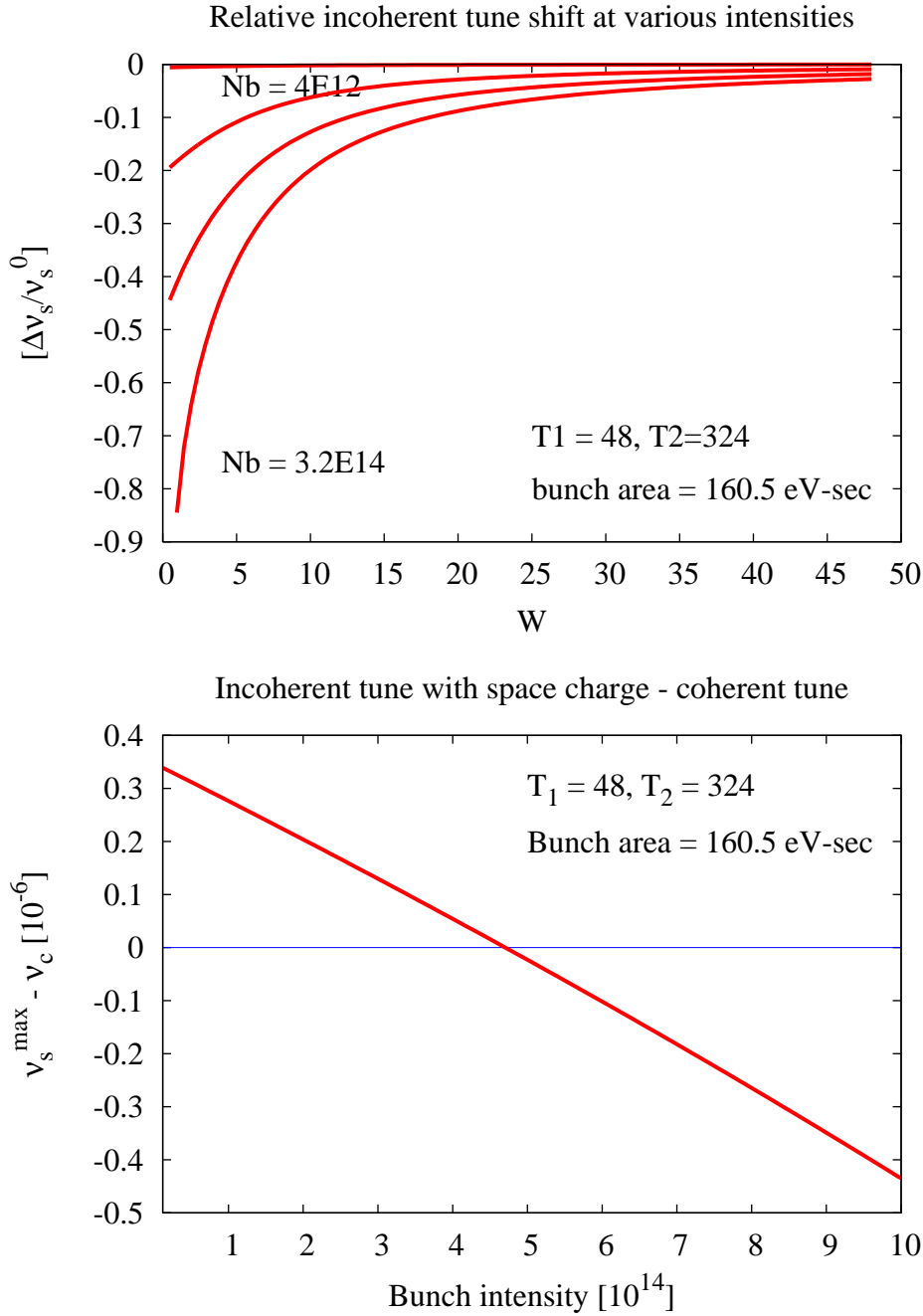


FIG. 9: Top: Relative difference of the incoherent tune with space charge and without space charge as a function of W , the barrier penetration at bunch intensities varying from $N_b = 4 \times 10^{12}$ to $N_b = 3.2 \times 10^{14}$. Bottom: Difference of the maximum incoherent tune with space charge and the coherent frequency (multiplied by 10^6) as a function of the bunch intensity. The zero crossing defines the threshold for the loss of Landau damping, here the threshold is $N_b = 4.7 \times 10^{14}$.

pulse since the tune is also smallest there. The incoherent frequency decreases as the intensity increases and at a threshold frequency, the maximum of the incoherent tune will equal the coherent frequency. At higher intensities, the coherent frequency will be outside the spread and Landau damping is lost. For the nominal value of $T_2 = 324$ 'bkts', this threshold is reached when the intensity exceeds 4.7×10^{14} , about 100 times higher than present intensities.

VI. INSTABILITY THRESHOLDS AT DIFFERENT BUNCH LENGTHS

It has been observed in the SPS that a region where the incoherent frequency as a function of amplitude has an extremum is associated with the appearance of a local instability [8]. In a barrier bucket, the maximum of the incoherent tune occurs when the ratio of the peak energy on the orbit to the bucket height is $\sqrt{T_2/(4T_1)}$, see Equation (12). If this ratio is greater than unity, as is the case for the nominal Recycler parameters $T_2/(4T_1) = 324/(4 \times 48)$, the maximum lies outside the bucket. The effects of this local instability are not present under normal operation but can be studied by changing the separation T_2 .

The energy acceptance or bucket height depends on the area under the voltage pulse $V_0 T_1$ but not on T_2 . If we change the bunch length by adiabatically changing T_2 , the bunch area will be preserved and the energy acceptance will also be constant. The bucket area however is determined by the bucket height and the value of T_2 . The value of T_2 when the bucket area just encloses the bunch area is

$$T_2^{min} = \frac{1}{2} \sqrt{\frac{|\eta| T_0}{2\beta^2 E_0 e V_0 T_1}} A_{bunch} - \frac{4}{3} T_1 \quad (76)$$

Lower bunch area leads to a lower value for T_2^{min} and hence allows a wider range of variation with $T_2 < 4T_1$.

These studies were carried out in the Recycler using protons. The beam cooling systems as well as the transverse dampers were turned off during the experiment. For these measurements, a bunch with much lower intensity than normal was injected - the initial bunch area was about 27 eV-sec compared to a more typical value of 100

eV-sec. The bunch was injected into a gap which was 84 Booster buckets long, i.e. $T_2 = 84$ 'bkts' (a 'bkt' = $0.01893\mu\text{sec}$). We chose $T_1 = 48$ bkts and pulse height of 1.8kV, these being the usual values during regular operation. Once equilibrium was reached after injection, beam intensity along with data from the wall current and Schottky monitors were recorded to establish the initial parameters. Subsequently the beam was expanded or compressed adiabatically by changing T_2 to different values of interest without changing T_1 .

Figure 10 shows the measured longitudinal profiles along with the fits by the *tanh* function. In all cases, the fit describes the measured profile quite well. One slight exception is for the shortest bunch with $T_2 = 14$ bkts where the fit at the center does not quite match the flatness of the measured profile. Furthermore, it cannot be explained by the wall current monitor saturation which occurs at a minimum of 5 times the bunch intensity used in this experiment. However the rising and falling edges match very well. These edges in the barrier pulses determine the coherent frequency, not the bunch profile in the center.

Assuming that the bunch area is preserved, compressing the bunch length increases the energy spread and conversely. Figure 11 shows the maximum energy spread deduced from the Schottky spectrum and the theoretical values (shown by the curve) assuming that the initial bunch area was conserved. There are discrepancies between the two, especially at the shortest $T_2 = 14$ bkts. Some of this can be attributed to measurement errors of the energy spread from the Schottky spectrum. It is also likely that several beam dynamics processes lead to an increase in bunch area and loss of particles as the gap T_2 was decreased. This is confirmed by the measured Schottky spectra for the different profiles shown in Figure 12. At the smallest values of T_2 , the energy spread exceeds the energy acceptance of 17.4 MeV. However the spectral amplitudes, shown in db, also show that the losses were of the order of 1%.

We now consider the coherent frequency and the ratio of this frequency to the maximum of the bare incoherent frequency as a function of the bunch length, using the energy spread and the fitted values of the parameters b, c for each of the bunch profiles shown in Figure 10. This ratio is shown in Figure 13. First, the ratio increases with

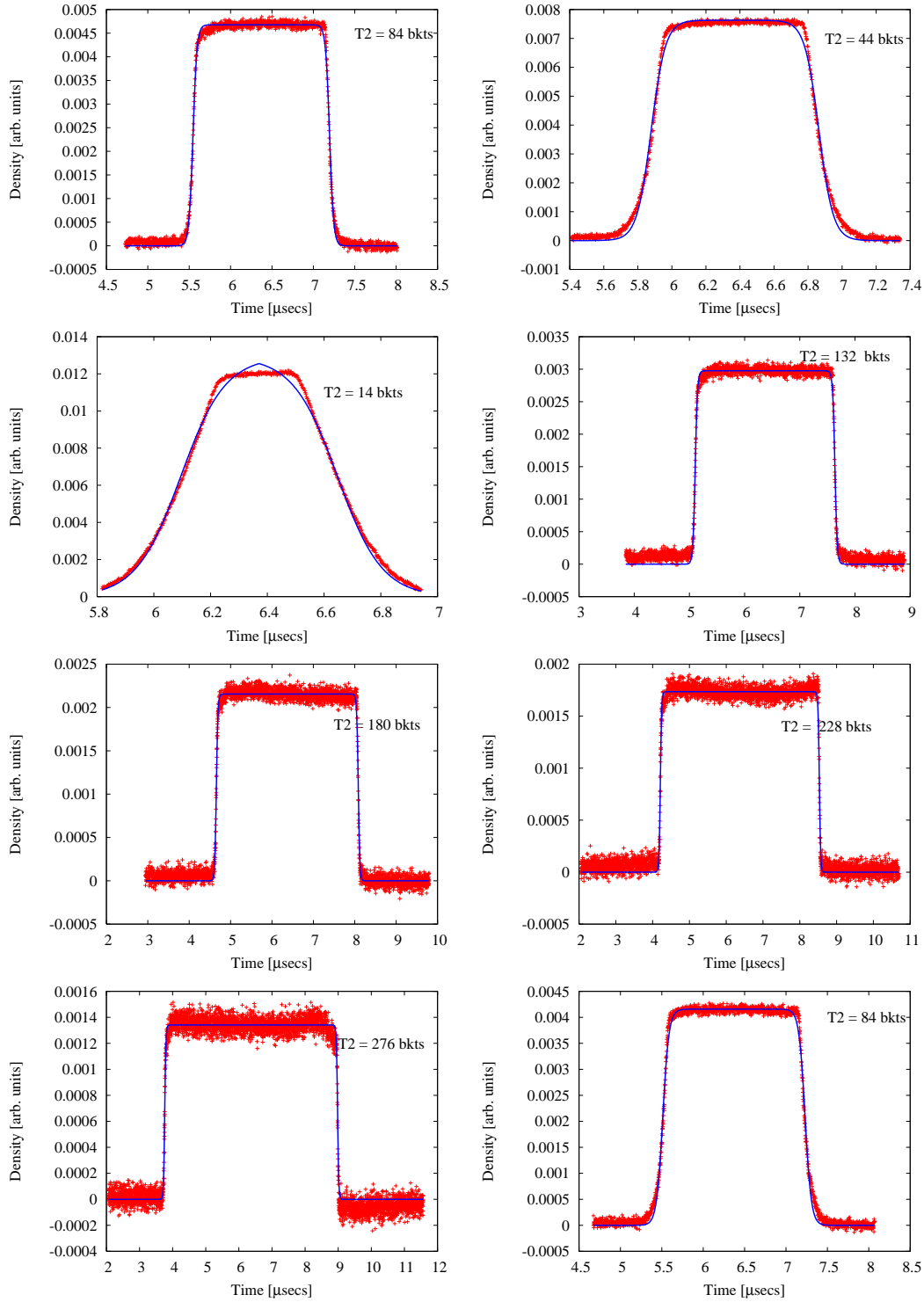


FIG. 10: Measured bunch profiles in March 2009. The value of T_2 was changed while T_1 was kept constant. The sequence of T_2 values is the measurement order. The measured data and the fits with the \tanh function are shown for the eight profiles.

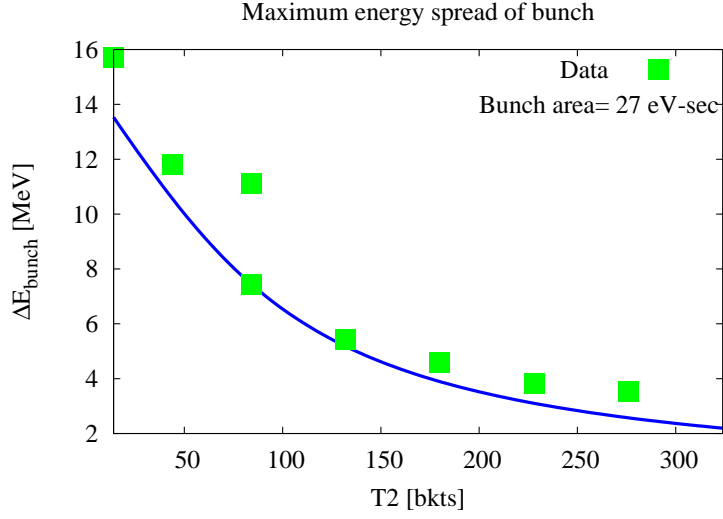


FIG. 11: The maximum energy spread as a function of T_2 . The data points are the values obtained from the Schottky spectrum while the curve shows the expected value assuming that the initial bunch area is preserved and no beam is lost. Over this range of T_2 from 14 bkts to 324 bkts, the maximum spread stays below the energy acceptance of 17.3 MeV. The deviations between the data and the curve show that the bunch area was not preserved, especially at the smallest value of $T_2 = 14$ bkts.

the bunch length or T_2 before falling at the largest value of T_2 . Note that both the coherent frequency and the maximum of the bare incoherent frequency *decrease* with T_2 . $\omega_{s0,max}$ decreases as $1/\sqrt{T_2}$ while the coherent frequency decreases at a slower rate, hence the ratio increases with T_2 . One would conclude from this observation that for bunches with the same (or nearly the same here) longitudinal emittance, shorter bunches have a higher threshold for the loss of Landau damping. Secondly, we observe that except for $T_2 = 14$, this ratio is greater than one implying that Landau damping was lost for most of the bunches in this study. This may explain some of the observed increase in bunch area.

Fig. 14 shows the surviving beam as a function of time. Various T_2 to T_1 ratios along with the beam lifetime are also indicated. There are three distinct regions in this plot. The first section had $T_2 < 4T_1$ with T_2 assuming values of 14, 44, 84, 130, 180

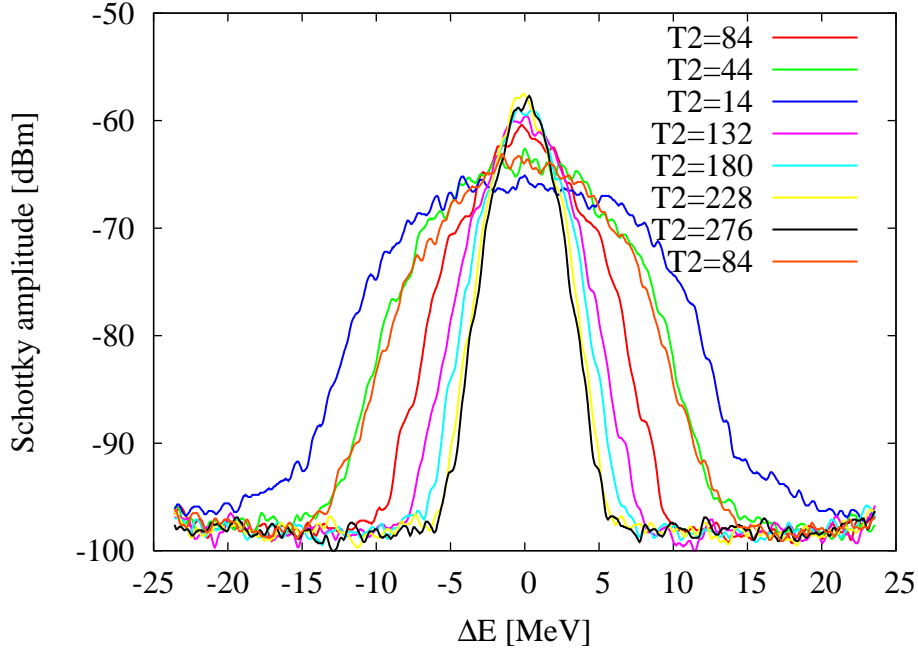


FIG. 12: Schottky spectra of bunches with different values of T_2 after background subtraction. At the smallest values of T_2 , the spectra extends beyond the energy acceptance suggesting that there was some beam loss but this amount was of the order of 1%.

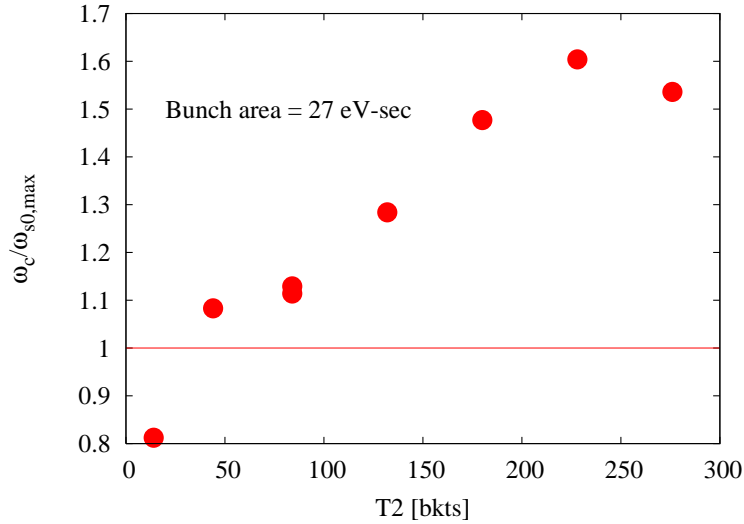


FIG. 13: Ratio of coherent to maximum of the bare incoherent frequency for the different bunches with line profiles shown in Figure 10.

bkts. The average lifetime of the beam at 8 hours was significantly lower than in the second section where it was about 50 hours with $T_2 = 228, 276$ and $> 4T_1$ in both cases. In the third region the beam was compressed to its original value of $T_2 = 84$ bkts. The lifetime again decreased by about a factor of two. There are many possible sources for these changes in lifetime as T_2 was changed: different energy spread, loss of Landau damping, local instability when $T_2 < 4T_1$, and possible resonance with the frequency of the Main Injector ramping. The density of particles at this resonant frequency changes with the bunch length and this resonance has been known to cause beam loss in the past. While we do not at present know the relative importance of these effects, the data is not inconsistent with the hypothesis that a local instability at the extremum of the incoherent synchrotron tune can contribute to beam loss. The effects of this instability are easily avoided in the barrier bucket by choosing appropriate values of T_1, T_2

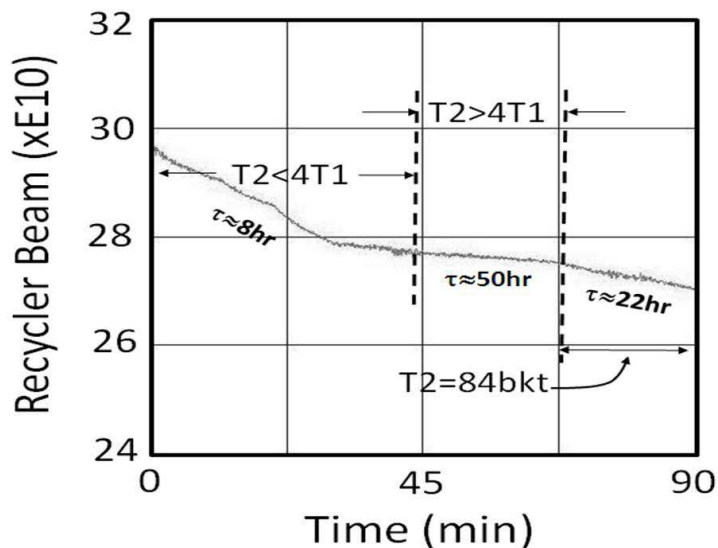


FIG. 14: Lifetime at various times with different T_2 to T_1 ratios.

VII. MICROWAVE INSTABILITY

So far we've only discussed the effect of the capacitive space charge impedance. However the Recycler also has a broadband resistive impedance with a cutoff at $f_c \sim c/b \approx 3.95$ GHz. At sufficiently high intensities, this resistive impedance can lead to asymmetric bunch shape distortion and eventually to turbulent bunch lengthening due to the onset of the microwave instability. While there is as yet no satisfactory theory of this instability for bunched beams, estimates for the threshold of the instability are made by using the coasting beam theory and replacing the beam current by the peak bunch current. For Gaussian bunches, the intensity threshold is given by

$$N_\mu = \sqrt{\frac{\pi}{2}} \frac{Z_0}{r_p} \frac{|\eta| \gamma}{\beta} \frac{\sigma_z \sigma_\delta^2}{|Z_{||}/n|} \quad (77)$$

We observe that for constant bunch area $A \sim \sigma_z \sigma_\delta$, the threshold $N_\mu \propto A^2/\sigma_z$. Hence for bunches of the same area, shorter bunches have a higher threshold.

As a preliminary estimate for the threshold of this instability, we will use the rms values of the energy spread and the bunch length for the measured distribution during normal operation. The rms energy spread is found from the Schottky spectrum while the rms bunch length can be found from

$$\tau_{rms} = \sqrt{a} \left[\int_{-(T_2/2+T_1)}^0 \tau^2 (1 + \tanh(b\tau + c)) d\tau + \int_0^{(T_2/2+T_1)} \tau^2 (1 - \tanh(b\tau - c)) d\tau \right]^{1/2}$$

For the fitted values of the parameters, we find $\tau_{rms} = 3.095\mu$ seconds while the rms energy spread is $\sigma_E = 4$ MeV. The effective wall impedance is estimated to be $Z_{||}/n = 1.6$ Ohms. Substituting the values we find that the bunch intensity threshold for the microwave instability is

$$N_\mu = 2.95 \times 10^{15} \quad (78)$$

This is about three orders of magnitude above present intensities. Space charge below transition does not induce the microwave instability but some results, e.g. [6] suggest that it may moderate the growth of the instability. Simulations may be necessary to understand this process.

VIII. CONCLUSIONS

Our primary findings are as follows:

- We considered two typical stationary phase space distributions as possible candidates for the Recycler: an elliptic distribution and an exponential (in the Hamiltonian) distribution. The first has an energy distribution which does not match observations while the second has a longitudinal profile distribution which does not match observations. In addition, both of these distributions are above the threshold for loss of Landau damping at present parameters.
- The longitudinal distribution that describes the Recycler bunches is a *tanh* distribution. This is found to be in very good agreement with observations made on separate days and with different beam parameters. This distribution was used to find the intensity at which the coherent dipole frequency is at the edge of the incoherent frequency distribution in the presence of space charge. This threshold for the loss of Landau damping is about two orders of magnitude above present intensities.
- An experiment to determine the impact of a local instability possibly induced at shorter bunch lengths was discussed. There are at least two competing mechanisms operating in this regime. On the one hand, at these bunch lengths the extremum of the incoherent frequency lies within the bunch frequency distribution and a local instability may develop. On the other hand we found that the threshold for the loss of Landau damping increases as the bunch is shortened with the area preserved. Nevertheless, beam loss was observed at shorter bunch lengths. Possible causes include higher energy spread, resonance with the Main Injector ramp frequency and perhaps the local instability.
- A rough estimate of the microwave instability threshold shows that in the absence of space charge, the threshold is about three orders of magnitude higher than present intensities. Table II shows the intensity thresholds from different effects.

Effect	Intensity threshold
Loss of Landau damping	4.7×10^{14}
Bucket height shrinks to 12 MeV	2.3×10^{15}
Microwave instability	2.9×10^{15}

TABLE II: Intensity thresholds for different effects, assuming $T_1 = 48$ bkts, $T_2 = 324$ bkts.

In a subsequent paper we will examine the stability diagrams in the presence of space charge and a resistive impedance. We will also report on results of simulations with a macro-particle tracking code (ESME) and a Vlasov code. The Vlasov code will be employed to compare with the intensity thresholds found in this paper as well as to understand the bunch behaviour following the onset of instability.

-
- [1] I. Gonzalez and F.Zimmermann, Proceedings of EPAC 2008 p. 1721 (2008).
 - [2] G. Jackson, Fermilab-TM-1991 (1996).
 - [3] J. E. Griffin, IEEE, Trans. Nucl., Sci. **NS-30**, 3502 (1983).
 - [4] C. M. Bhat, FERMILAB-CONF-06-102-AD **KEK Proceedings 2006-12**, 45 (2006).
 - [5] S. Y. Lee and K. Y. Ng, Phys. Rev. E **56**, 5992 (1997).
 - [6] O. Boine-Frankenheim and I. Hofmann, Phys. Rev. ST AB **6**, 034207 (2003).
 - [7] A. Hofmann and F. Pedersen, IEEE Trans. Nucl. Sci. **26**, 3526 (1979).
 - [8] E. Shaposhnikova, T. Bohl, and T. Linnecar, Proceedings of PAC05 p. 2300 (2005).